J Physiol Sci (2010) 60:205–212
DOI 10.1007/s12576-010-0086-y

ORIGINAL PAPER

Right ventricular stiffness constant as a predictor of postoperative hemodynamics in patients with hypoplastic right ventricle: a theoretical analysis

Shuji Shimizu · Toshiaki Shishido · Dai Une · Atsunori Kamiya · Toru Kawada · Shunji Sano · Masaru Sugimachi

Received: 9 December 2009 / Accepted: 10 January 2010 / Published online: 4 February 2010

Abstract One and a half ventricle repair (1.5VR) is a surgical option for hypoplastic right ventricle (RV). The benefits of this procedure compared to biventricular repair (2VR) or Fontan operation remain unsettled. To compare postoperative hemodynamics, we performed a theoretical analysis using a computational model based on lumped-parameter state-variable equations. We varied the RV stiffness constant (B_{RV}) to simulate the various RV hypoplasia, and estimated hemodynamics for a given B_{RV}. With $B_{RV} < 150\%$ of normal, cardiac output was the largest in 2VR. With $B_{RV} > 150\%$, cardiac output became larger in 1.5VR than in 2VR. With $B_{RV} > 250\%$, RV end-diastolic volume was almost the same between 1.5VR and 2VR, and a rapid increase in atrial pressure precluded the use of 1.5VR. These results indicate that the beneficial effect of 1.5VR depends on the RV stiffness constant. Determination of management strategy should not only be based on the morphologic parameters but also on the physiological properties of RV.

S. Shimizu (✉) · T. Shishido · D. Une · A. Kamiya · T. Kawada · M. Sugimachi
Department of Cardiovascular Dynamics, Advanced Medical Engineering Center, National Cardiovascular Center Research Institute, 5-7-1 Fujishiro-dai, Suita, Osaka 565-8565, Japan
e-mail: shujismz@ri.ncvc.go.jp

S. Shimizu · S. Sano
Department of Cardiovascular Surgery, Okayama University Graduate School of Medicine, Dentistry and Pharmaceutical Sciences, Okayama, Japan

S. Shimizu
Japan Association for the Advancement of Medical Equipment, Tokyo, Japan

Keywords One and a half ventricle repair · Right ventricular stiffness · Hypoplastic right ventricle · Computational model

Introduction

One and a half ventricle repair (1.5VR) is a surgical option for hypoplastic right ventricle (RV) caused by various congenital heart diseases including pulmonary atresia with intact ventricular septum (PA/IVS), Ebstein's anomaly or their relatives. In this procedure, the superior vena cava (SVC) is directly connected to the pulmonary artery (PA). Therefore, the blood from SVC directly enters PA, whereas the blood from the inferior vena cava (IVC) is pumped by RV to PA. This procedure is clinically acceptable because of its low surgical risk [1, 2]. However, the benefits of this procedure on postoperative hemodynamics in patients with a wide spectrum of RV hypoplasia compared to other procedures such as biventricular repair (2VR) and Fontan operation remain unsettled [3]. Furthermore, conversion to Fontan circulation was required late after 1.5VR in a possibly inappropriate candidate [4].

Although various authors reported an arbitrary selection scheme for the procedures based on RV morphology such as RV end-diastolic volume (RVEDV) [1, 2, 5], the long-term outcomes of 1.5VR have remained insufficiently known [5]. The previous criteria do not likely predict postoperative hemodynamics of these complex circulations accurately because morphological values measured preoperatively largely depend on the RV preload and afterload conditions, which change remarkably between subjects and between before and after the operation.

Hypoplastic RV is physiologically characterized by increased RV stiffness, caused by hypertrophy and

fibroelastosis of RV muscles [6]. However, how RV stiffness influences the postoperative hemodynamics has not been reported. Given the small number of patients with each of the wide variety of preoperative RV conditions [7, 8], the influence of RV stiffness on 1.5VR, 2VR, and Fontan operation cannot be examined by clinical study. It is also difficult to experimentally reproduce hemodynamics before and after 1.5VR for hypoplastic RV with various stiffness. In view of the above, we attempted to clarify postoperative hemodynamics by a theoretical analysis using a computational model based on lumped-parameter state-variable equations. The present results indicate that the RV stiffness constant may provide selection criteria for 1.5VR.

Materials and methods

The electrical analogs of the model used to simulate the cardiovascular system are shown in Fig. 1. We modeled the postoperative cardiovascular system mathematically by a combination of the time-varying elastance cardiac chamber model and the three-element Windkessel vascular model. We set the normal values of parameters to be appropriate for a 75-kg man. These values were obtained from the literature [9–13] and are listed in Table 1. Since the data of the pressure–volume relationship of the atrium were scarcely available, parameters of the atrium were surmised from the literature [10–12].

Heart

The right and left ventricular chambers as well as the atrial chambers are represented by the time-varying elastance model [9, 10, 13]. The end-systolic pressure–volume relationship is described by a linear formula:

$$P_{es,cc} = E_{es,cc}\left[V_{es,cc} - V_{0,cc}\right] \quad (1)$$

where $P_{es,cc}$ and $V_{es,cc}$ are end-systolic pressure and volume, respectively; $E_{es,cc}$ is the maximal volume elastance; $V_{0,cc}$ is the volume at which $P_{es,cc}$ is equal to 0 mmHg. cc denotes each chamber, i.e., RA for the right atrium, LA for the left atrium, RV for the right ventricle, or LV for the left ventricle. The end-diastolic pressure–volume relationship is represented by a non-linear formula:

$$P_{ed,cc} = A_{cc}\left[e^{B_{cc}(V_{ed,cc}-V_{0,cc})} - 1\right] \quad (2)$$

where $P_{ed,cc}$ and $V_{ed,cc}$ are end-diastolic pressure and volume, respectively; A_{cc} and B_{cc} are constants [9, 10, 13]. We assumed the time course of the time-varying elastance by defining normalized elastance curve $e_{cc}(t)$ as:

Table 1 Parameters used in modeling

Heart rate (HR), beats/min	75			
Duration of cardiac cycle (T_c), ms	800			
Time advance of atrial systole (DT), ms	16			
Total stressed blood volume (V_s), ml	750	(control only)		
	LV	RV	LA	RA
Time to end systole (T_{es}), ms	200	200	120	120
End-systolic elastance (E_{es}), mmHg/ml	3.0	0.7	0.5	0.5
Scaling factor of EDPVR (A), mmHg	0.35	0.35	0.06	0.06
Exponent scaling factor for EDPVR (B), ml^{-1}	0.033	0.023	0.264	0.264
Unstressed volume (V_0), ml	0	0	5	5
	Aortic	Pulmonary	Mitral	Tricuspid
Valvular resistance (forward), (mmHg s)/ml	0.001	0.001	0.001	0.001
	Systemic		Pulmonary (p)	
	Superior (ss)	Inferior (si)		
Arterial resistance (R_a), (mmHg s)/ml	2.25	1.5	0.03	
Characteristic impedance (R_c), (mmHg s)/ml	0.075	0.05	0.02	
Venous resistance (R_v), (mmHg s)/ml	0.0375	0.025	0.015	
Arterial capacitance (C_a), ml/mmHg	0.528	0.792	13	
Venous capacitance (C_v), ml/mmHg	28	42	8	

LV Left ventricle, *RV* right ventricle, *LA* left atrium, *RA* right atrium, *EDPVR* end-diastolic pressure–volume relationship

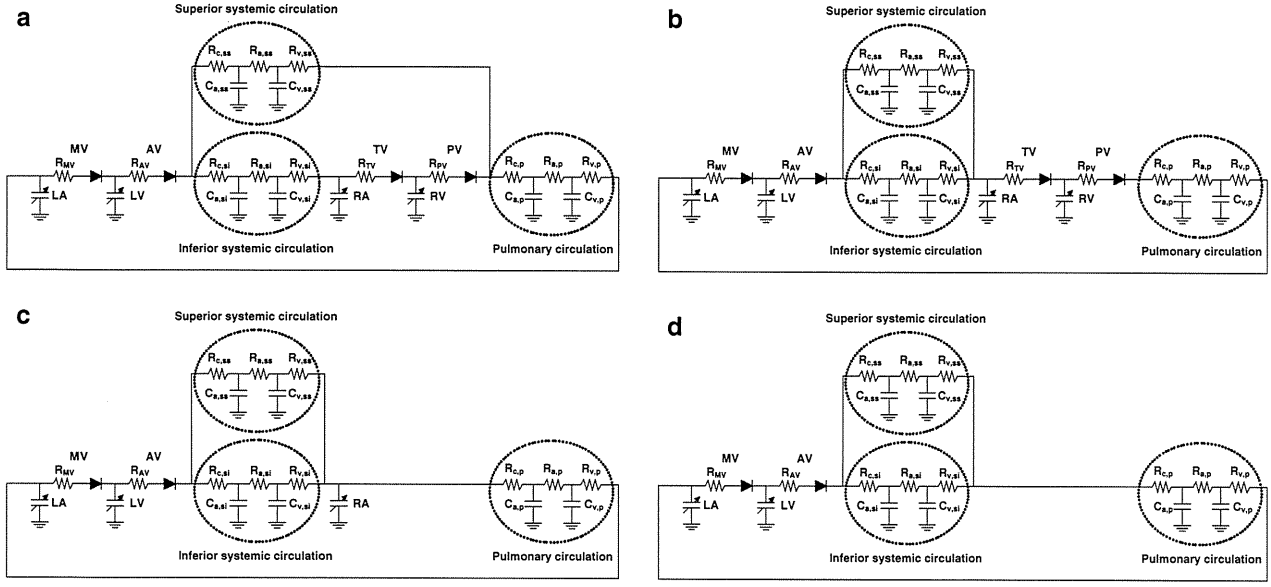

Fig. 1 **a** The electric equivalent circuit of one and a half ventricle repair. **b** Biventricular repair (normal circulation). **c**,**d** Variations of Fontan operation [**c** atriopulmonary connection (APC); **d** total cavopulmonary connection (TCPC)]. *LV* and *RV* left and right ventricles, *LA* and *RA* left and right atria, *AV* and *MV* aortic and mitral valves, *PV* and *TV* pulmonary and tricuspid valves, C_a and C_v lumped arterial and venous capacitances, R_c characteristic impedances, R_a lumped arterial resistances, R_v venous resistances, *ss* superior systemic circulation, *si* inferior systemic circulation, *p* pulmonary circulation

$$e_{cc}(t) = 0.5[1 - \cos(\pi t/T_{es,cc})]\ (0 \le t < 2T_{es,cc})$$
$$e_{cc}(t) = 0\ (2T_{es,cc} \le t < T_c) \quad (3)$$

where t is the time from the start of systole, $T_{es,cc}$ is the duration of systole, and T_c is the duration of cardiac cycle. Using $e_{cc}(t)$, the instantaneous pressure, $P_{cc}(t)$, is described by:

$$P_{cc}(t) = [P_{es,cc}(V_{cc}) - P_{ed,cc}(V_{cc})]e_{cc}(t) + P_{ed,cc}(V_{cc}) \quad (4)$$

Ventricular systole is preceded by atrial systole. The time advance of atrial systole (DT) is calculated as the fixed fraction of T_c (DT = $0.02T_c$). Function of each chamber is characterized by the parameters $E_{es,cc}$, $T_{es,cc}$, $V_{0,cc}$, A_{cc}, B_{cc}, and $e_{cc}(t)$. The same $e_{cc}(t)$ was used for all chambers, but the other parameters were different between chambers, as shown in Table 1.

Vascular system

Basically, the pulmonary and systemic circulations are modeled as modified Windkessel impedances. Each vascular system is modeled by lumped venous (C_v) and arterial (C_a) capacitances, a characteristic impedance (R_c) that is related to the stiffness of the proximal aorta or pulmonary artery, a lumped arterial resistance (R_a), and a resistance proximal to C_v (R_v). This framework is similar to that used in deriving Guyton's resistance to venous return [14].

To simulate the postoperative hemodynamics of 1.5VR, the systemic circulation is divided into two parts, the superior and the inferior circulation. Therefore, the parameters of the systemic circulation are also divided into the superior and inferior ones, as shown in Fig. 1. Blood flow in the descending aorta is reported to be 63.8% of the left ventricular output [15]. The compliance of the IVC is considered to be 66.6% of the total venous compliance [16]. Thus, in our model, arterial and venous compliances of the inferior systemic circulation are adjusted to 0.6 times those of the compliance of the total circulation, and the blood flow of the inferior systemic circulation is controlled to be 60% of the left ventricular output by adjusting the resistances of R_c, R_a, and R_v.

The capacitance of the superior systemic circulation is also divided into arterial ($C_{a,ss}$) and venous ($C_{v,ss}$). Similarly, arterial and venous capacitances are defined for the inferior systemic circulation ($C_{a,si}$ and $C_{v,si}$) and for the pulmonary circulation ($C_{a,p}$ and $C_{v,p}$). The ratio of C_a to C_v was obtained from the literature [9, 10, 13]. The relationship between pressure (P_c) and volume (V_c) in each capacitance is described by the following linear formula.

$$P_c = \frac{V_c}{C} \quad (5)$$

The changes in volume in each capacitance ($dV(t)/dt$) are described by the differential equations below

$$\frac{dV(t)}{dt} = \sum Q_{\text{in-flow}}(t) - \sum Q_{\text{out-flow}}(t) \quad (6)$$

where $\Sigma Q_{\text{in-flow}}(t)$ and $\Sigma Q_{\text{out-flow}}(t)$ indicate the sum of instantaneous volumetric flow rates at the inlet and outlet of each compartment, respectively. Each of the aortic, mitral, pulmonary, and tricuspid valves is described as an ideal diode with a serially connected small resistor.

In the 1.5VR model, the superior circulation flows from SVC to PA, while the inferior blood flow returns to RA through IVC as shown in Fig. 1a. The models of 2VR (Fig. 1b) and variations of Fontan operation [Fig. 1c, atriopulmonary connection (APC); Fig. 1d, total cavopulmonary connection (TCPC)] are constructed for comparisons. Although the superior and inferior systemic circulations return to RA in both 2VR and APC models, RA is directly connected to PA in the APC model. In the TCPC model, SVC and IVC are directly connected to PA. All parameter values were the same for all of these models except total stressed blood volume (see below) (Table 1).

Hypoplastic RV

Hypoplastic RV is physiologically characterized by an increase in RV stiffness caused by hypertrophy and fibroelastosis of RV muscles [6]. Recalling Eq. 2 for RV, we have:

$$P_{\text{ed,RV}} = A_{\text{RV}}\left[e^{B_{\text{RV}}\left(V_{\text{ed,RV}} - V_{0,\text{RV}}\right)} - 1\right] \quad (7)$$

where B_{RV} is stiffness constant of RV. The value of B_{RV} was changed stepwise from 0.023/ml (normal RV) to 0.143/ml (extremely stiff RV) in increments of 0.01/ml to simulate the various degrees of RV stiffness associated with hypoplasia (Fig. 2).

Protocols

First, the control state was simulated by the 2VR model with normal RV stiffness constant ($B_{\text{RV}} = 0.023$). The total stressed blood volume (V_s), equal to the sum of the stressed volumes in each capacitance and the volume of each chamber, was set as 750 ml to reproduce normal hemodynamics.

$$V_s = V_{\text{LV}} + V_{\text{RV}} + V_{\text{LA}} + V_{\text{RA}} + V_{\text{Ca,ss}} + V_{\text{Cv,ss}} + V_{\text{Ca,si}} + V_{\text{Cv,si}} + V_{\text{Ca,p}} + V_{\text{Cv,p}} \quad (8)$$

We solved these simultaneous equations (Eqs. 1–8) using the component ODE45 of MATLAB, based on the Runge–Kutta method (MathWorks). The hemodynamic parameters of 2VR with normal RV stiffness constant are listed in Table 2.

Next, systemic cardiac output, pulmonary arterial pressure (PAP), right atrial pressure (RAP), and RVEDV after each procedure were calculated for each RV stiffness constant. Heart rate was kept constant and mean systemic arterial pressure (MAP) was controlled at the same value as that of the control state, by adjusting the total stressed blood volume.

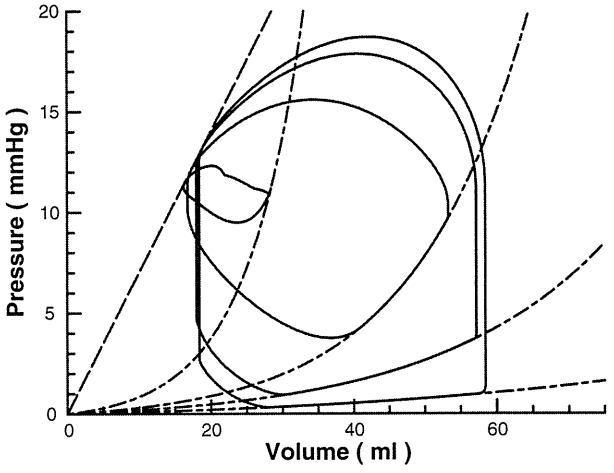

Fig. 2 Right ventricular pressure–volume loops (PV loop) after one and a half ventricle repair. With the increase in the right ventricular stiffness constant, the PV loop became smaller. The *horizontal axis* is the instantaneous right ventricular volume (ml) and the *longitudinal axis* is the instantaneous right ventricular pressure (mmHg)

Table 2 Control hemodynamic parameters (2VR with normal RV stiffness constant)

Parameter	Value
Heart rate (HR), beats/min	75
Mean systemic arterial pressure (MAP), mmHg	80.3
Mean pulmonary arterial pressure (PAP), mmHg	13.6
Mean right atrial pressure (RAP), mmHg	2.34
Mean left atrial pressure (LAP), mmHg	8.26
Left ventricular cardiac output (CO), l/min	4.95

Results

Figure 3a shows the impact of the RV stiffness constant on systemic cardiac output after each procedure. In the Fontan circulation (APC and TCPC), systemic cardiac output was independent of the RV stiffness constant and remained at 4.40 l/min. Under the condition of normal RV stiffness constant, systemic cardiac output was 4.95 l/min in 2VR and 4.73 l/min in 1.5VR, being 13 and 8% greater than that of Fontan circulation, respectively. As the RV stiffness constant was increased from the control value to mimic increased severity of RV

hypoplasia, systemic cardiac output decreased in both 2VR and 1.5VR circulations. Within the range between 100 and 150% of the control RV stiffness constant, systemic cardiac output of 2VR circulation was obviously greater than those of other two circulations. With the RV stiffness constant >150%, systemic cardiac output became greater in 1.5VR than in 2VR. In this situation, 2VR needed larger stressed blood volume than 1.5VR to maintain MAP (Fig. 3d).

The results for PAP and RAP are shown in Fig. 3b. As the RV stiffness constant increased, PAP decreased and RAP increased in both 2VR and 1.5VR circulations. In 2VR circulation, RAP increased steeply as the RV stiffness constant increased up to 150% of normal, and exceeded the atrial pressure of TCPC when the RV stiffness constant increased above 150% of normal. In 1.5VR circulation, RAP also increased but more slowly and exceeded the atrial pressure of TCPC only when the RV stiffness constant increased above 250% of normal. PAP in 1.5VR circulation, which was equal to SVC pressure, became higher than PAP in 2VR circulation in the range of RV stiffness constant >150% of normal.

In the control state, RVEDV in 2VR was 87.7 ml, which was treated as the value of 100% of RVEDV. The influence of the RV stiffness constant on RVEDV is shown in Fig. 3c. In 2VR circulation, RVEDV decreased as the RV stiffness constant increased. In 1.5VR circulation, RVEDV reduced only slightly with an increase in the RV stiffness constant until 250% of normal. In the range of RV stiffness constant >250% of normal, RVEDV showed a relatively linear decay in both 2VR and 1.5VR circulations, and there was no difference in RVEDV between 2VR and 1.5VR. In this situation, both 1.5VR and 2VR needed larger stressed blood volume than Fontan circulation (Fig. 3d).

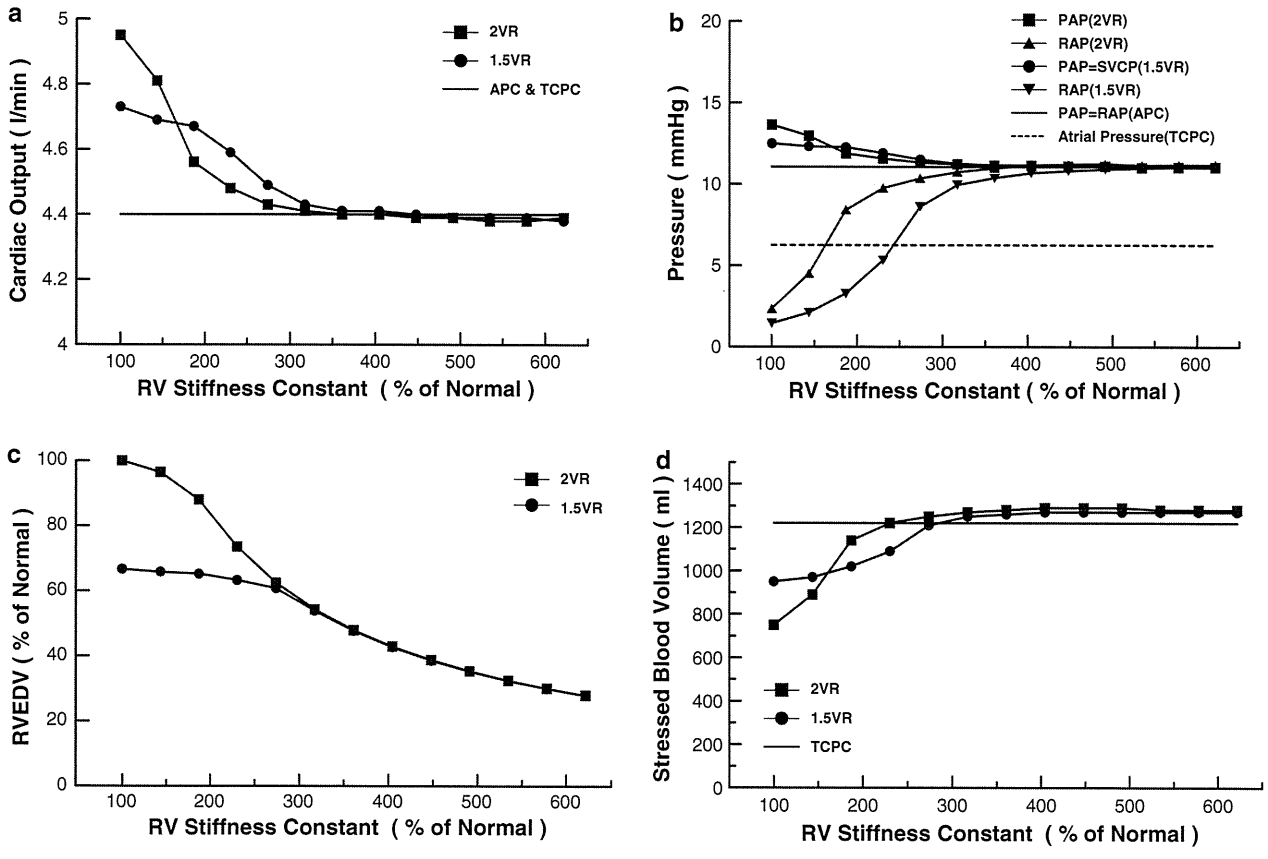

Fig. 3 **a** The relationship between systemic cardiac output (l/min) and % stiffness constant of hypoplastic right ventricle. The *horizontal axis* is the ratio of RV stiffness constant (% stiffness constant) to the normal value. **b** The relationship between pulmonary arterial pressure or right atrial pressure (mmHg) and % stiffness constant of hypoplastic RV. Pulmonary arterial pressure is the same as right atrial pressure in APC. **c** The relationship between % RVEDV and % stiffness constant of hypoplastic RV. **d** The relationship between stressed blood volume (ml) and % stiffness constant. *2VR* biventricular repair, *1.5VR* one and a half ventricle repair, *APC* and *TCPC* variations of Fontan operation (*APC* atriopulmonary connection, *TCPC* total cavopulmonary connection); *PAP* pulmonary arterial pressure, *RAP* right atrial pressure, *SVCP* superior vena caval pressure, *RVEDV* right ventricular end-diastolic volume

Discussion

The results of this theoretical analysis suggest that, in patients with hypoplastic RV, postoperative hemodynamics depends largely on the RV stiffness constant. PA/IVS, Ebstein's anomaly or their relatives are characterized by varying degrees of underdevelopment of RV. For a severely hypoplastic RV, the definitive treatment is single ventricular circulation. For a mildly hypoplastic RV, biventricular circulation is expected to have merit. Recently, 1.5VR has been proposed to reduce the surgical risk of 2VR. The use of 1.5VR has lowered the early or midterm mortality, and adequate growth of RV and the tricuspid valve has been documented in some patients [2]. However, the postoperative RV dysfunction or arrhythmic event has also been reported, in particular, when the patients are on the borderline of criteria between 1.5VR and Fontan operation [4, 5].

For the choice of surgical options among Fontan operation, 1.5VR, and 2VR, the previously used criteria were based on morphologic characteristics of the hypoplastic RV, such as RVEDV. However, simple anatomic indices may be inaccurate, since these values are dependent on the afterload and preload conditions. For that reason, the treatment strategy for hypoplastic RV based on the anatomic indices remains controversial. We focused on the intrinsic property of hypoplastic RV, i.e., RV stiffness constant. The fact that the RV stiffness constant, an index of chamber property, is relatively independent of the loading condition is important for the accurate prediction of postoperative hemodynamics. Based on the results of the present study, we propose that patients with hypoplastic RV can be classified into three groups according to the RV stiffness constant. The first group consists of patients with mild RV hypoplasia (RV stiffness constant <150% of normal), in whom enlargement of RV is expected after the operation. At the other extreme, the second group consists of patients with severe RV hypoplasia (RV stiffness constant >250%), in whom no RV reconstruction is expected to have merit. In addition, we have shown that there certainly exists a third group consisting of patients with intermediate RV hypoplasia (RV stiffness constant between 150 and 250%), who would benefit more from 1.5VR than from 2VR or Fontan operation.

Mild RV hypoplasia

When RV hypoplasia is mild (RV stiffness constant <150% of normal), systemic cardiac output is greater in 2VR than in 1.5VR or Fontan operation (APC or TAPC). Therefore, we recommend that 2VR should be chosen in the mild RV hypoplasia group. Although systemic cardiac output in 1.5VR is also greater than that in Fontan operation, SVC pressure (which is equal to PAP) is higher than that of APC. Accordingly, the upper part of the body is exposed to higher SVC pressure in 1.5VR, which may cause postoperative pleural effusion [2]. A large pressure gradient between SVC and IVC also results in abnormal venous collaterals from SVC to IVC [17–20], and they could effectively increase the venous return to RA in 1.5VR.

Intermediate RV hypoplasia

When RV hypoplasia is intermediate (RV stiffness constant between 150 and 250% of normal), systemic cardiac output in 1.5VR exceeds that in 2VR. Although SVC pressure is still higher in 1.5VR than in APC, RAP is lower in 1.5VR than in the other procedures. This condition is favorable to reduce supraventricular arrhythmias related to high RAP during the perioperative periods. This beneficial effect is not expected for 2VR since RAP in 2VR is higher than the atrial pressure of TCPC. Furthermore, 1.5VR is advantageous from the viewpoint of stressed blood volume because 1.5VR needs smaller stressed blood volume than does 2VR to maintain MAP (Fig. 3d).

In these patients, RVEDV in 1.5VR is relatively independent of the RV stiffness constant. However, abnormal systemic venous collateral channels might open after 1.5VR. These collateral channels would increase RV preload wastefully and decrease systemic cardiac output in the late postoperative phase. In such conditions, conversion to the Fontan circulation may be required in the late phase [4, 5]. Nevertheless, 1.5VR should be recommended for the intermediate RV hypoplasia group because high cardiac output and low RAP are anticipated.

Severe RV hypoplasia

When RV hypoplasia is severe (RV stiffness constant >250% of normal), neither 1.5VR and 2VR are expected to improve systemic cardiac output. In this condition, RVEDV is almost the same between 1.5VR and 2VR, and linearly decreases with an increase in the RV stiffness constant in spite of a rapid elevation in RAP. This indicates that RVEDV might be independent of the venous return to RA. Since RAP becomes higher than the atrial pressure of TCPC even in 1.5VR, supraventricular arrhythmias caused by high RAP are liable to occur [2, 5]. In this condition, 1.5VR is considered to have hemodynamics equivalent to APC and needs larger stressed blood volume than does TCPC to maintain systemic arterial pressure (Fig. 3d).

Therefore, TCPC should be chosen for patients with severe RV hypoplasia. In these patients, the arrhythmic events after TCPC are less than that after APC [21, 22]. Although a small pressure gradient between SVC and IVC

remains in 1.5VR, this may not be of clinical significance. Systemic venous collateral channels are expected to be rare, and an increase of RV volume after the operation is unlikely.

Clinical implication

The management strategy for patients with hypoplastic RV has been based on the morphological characteristics, which are dependent on the loading conditions. In contrast, we used a relatively load-independent index, RV stiffness constant, and simulated the postoperative hemodynamics. As a result, we identified the characteristics of hemodynamics after each of the surgical options, and clearly defined the indications of these operations.

Moreover, our results may be useful to theoretically speculate the reason for contrasting clinical findings. Chowdhury and colleagues [2] reported that the event rate of supraventricular arrhythmia was about 15% in the late postoperative phase of 1.5VR. On the other hand, Numata et al. [5] reported higher arrhythmic event rate. In the former report, the patients had a relatively high postoperative RV volume (45–75% of predicted normal RV; Fig. 3c) and a large pressure gradient between SVC and IVC (mean 7.6 mmHg; Fig. 3b) after 1.5VR. Indeed, there was significant pleural effusion in 22.7% of patients. Our results suggest that good systemic cardiac output, low IVC pressure, and high SVC pressure after 1.5VR can be expected under a condition of a relatively small RV stiffness constant. A great difference between SVC and IVC pressures may cause pleural effusion. Therefore, patients in the former report are likely to have low RV stiffness. In the latter report, the average RVEDV at 1 year after 1.5VR was about 50% of normal and there was no obvious collateral after the surgery in the patients examined. These data suggest a high RV stiffness (Fig. 3c), and a small difference between SVC and IVC pressures (Fig. 3b). Since higher arrhythmic event rate is likely to be associated with high RAP in patients with high RV stiffness, we can interpret the marked difference in arrhythmic event rate in these studies based on postoperative hemodynamics. Operations with 1.5 VR in potentially inappropriate patients (i.e., patients with stiffer RV) might impair long-term outcomes by continued high RAP-induced arrhythmia.

If we can assess the RV stiffness constant and other hemodynamic data in a catheter laboratory before operation, we will be able to select the most suitable operation for patients with hypoplastic RV. Recently, noninvasive methods for predicting LV chamber stiffness using echocardiography have been reported [23–25]. For example, LV chamber stiffness has been estimated from the deceleration time of LV early filling, effective mitral area and length. Such a method may be applied to estimate RV chamber stiffness using the deceleration time of RV early filling, effective tricuspid area and length. Moreover, it may be possible to choose an appropriate procedure for individual patients by performing simulation of postoperative hemodynamics from individual data using our model. Further clinical studies are needed to precisely assess the RV stiffness constant, including the above methods.

Limitations

A major limitation of this study is related to the parameters we used for the model. In our model, all parameters other than the RV stiffness constant are fixed. It is reported that RV end-systolic elastance as well as the RV stiffness constant depend upon RV histological changes such as RV hypertrophy [26]. The increase in RV end-systolic elastance moves the beneficial range of 1.5VR toward the stiffer range of the RV stiffness constant. The increase of heart rate also moves the range toward the stiffer range (Table 3). Moreover, ischemia caused by long-standing hypoxemia and hypertension of RV may influence other variables [6]. The existence of pulsatility of the pulmonary circulation may also affect the pulmonary vascular resistance [27]. Tricuspid regurgitation may also impair the postoperative hemodynamics. These limitations may be solved by using the preoperative data of individual patients. Santamore and Burkhoff have already reported the importance of ventricular interdependence using a computer model [13]. However, ventricular interdependence between small hypoplastic RV and relatively large left ventricle may be negligible.

Table 3 The influence of right ventricular end-systolic elastance and heart rate on the beneficial range of the one and a half ventricle repair

	Lower limit of RV stiffness constant (% of normal)	Upper limit of RV stiffness constant (% of normal)
$E_{es,RV} = 0.7$, HR = 75	150	250
$E_{es,RV} = 1.4$, HR = 75	200	300
$E_{es,RV} = 0.7$, HR = 100	175	275

RV Right ventricle, $E_{es,RV}$ right ventricular end-systolic elastance (mmHg/ml), *HR* heart rate (beats/min)

Conclusion

Using a model analysis, we have shown that the beneficial effect of 1.5VR depends on the RV stiffness constant. 1.5VR is the most beneficial for hypoplastic RV with 150–250% of normal RV stiffness constant. The beneficial range of 1.5VR may also be changed by individual parameters other than the RV stiffness constant, but the beneficial range certainly exists. Therefore, determination of management strategy should be based not only on the morphologic parameters but also on the physiologically determined properties.

Acknowledgments This study was supported by Health and Labor Sciences Research Grants (H18-nano-Ippan-003, H19-nano-Ippan-009, H20-katsudo-Shitei-007 and H21-nano-Ippan-005) from the Ministry of Health, Labor and Welfare of Japan, by Grants-in-Aid for Scientific Research (No. 20390462) from the Ministry of Education, Culture, Sports, Science and Technology in Japan, and by the Industrial Technology Research Grant Program from New Energy and Industrial Technology Development Organization (NEDO) of Japan.

References

1. Yoshimura N, Yamaguchi M, Ohashi H, Oshima Y, Oka S, Yoshida M, Murakami H, Tei T (2003) Pulmonary atresia with intact ventricular septum: strategy based on right ventricular morphology. J Thorac Cardiovasc Surg 126:1417–1426
2. Chowdhury UK, Airan B, Talwar S, Kothari SS, Saxena A, Singh R, Subramaniam GK, Juneja R, Pradeep KK, Sathia S, Venugopal P (2005) One and one-half ventricle repair: results and concerns. Ann Thorac Surg 80:2293–2300
3. Hanley FL (1999) The one and a half ventricle repair-we can do it, but should we do it? J Thorac Cardiovasc Surg 117:659–661
4. Uemura H, Yagihara T, Adachi I, Kagisaki K, Shikata F (2007) Conversion to total cavopulmonary connection after failed one and one-half ventricular repair. Ann Thorac Surg 84:666–668
5. Numata S, Uemura H, Yagihara T, Kagisaki K, Takahashi M, Ohuchi H (2003) Long-term functional results of the one and one half ventricular repair for the spectrum of patients with pulmonary atresia/stenosis with intact ventricular septum. Eur J Cardiothorac Surg 24:516–520
6. Freedom RM (1998) Pulmonary atresia with intact ventricular septum—the significance of the coronary arterial circulation. In: Redington AN, Brawn WJ, Deanfield JE, Anderson RH (eds) The right heart in congenital heart disease. Greenwich Medical Media, London
7. Hanley FL, Sade RM, Blackstone EH, Kirklin JW, Freedom RM, Nanda NC (1993) Outcomes in neonatal pulmonary atresia with intact ventricular septum. A multiinstitutional study. J Thorac Cardiovasc Surg 105:406–427
8. Ashburn DA, Blackstone EH, Wells WJ, Jonas RA, Pigula FA, Manning PB, Lofland GK, Williams WG, McCrindle BW, Congenital Heart Surgeons Study members (2004) Determinants of mortality and type of repair in neonates with pulmonary atresia and intact ventricular septum. J Thorac Cardiovasc Surg 127:1000–1007
9. Burkhoff D, Tyberg JV (1993) Why does pulmonary venous pressure rise after onset of LV dysfunction: a theoretical analysis. Am J Physiol 265:H1819–H1828
10. Morley D, Litwak K, Ferber P, Spence P, Dowling R, Meyns B, Griffith B, Burkhoff D (2007) Hemodynamic effects of partial ventricular support in chronic heart failure: results of simulation validated with in vivo data. J Thorac Cardiovasc Surg 133:21–28
11. Goodwin JA, van Meurs WL, Sá Couto CD, Beneken JE, Graves SA (2004) A model for educational simulation of infant cardiovascular physiology. Anesth Analg 99:1655–1664
12. Migliavacca F, Pennati G, Dubini G, Fumero R, Pietrabissa R, Urcelay G, Bove EL, Hsia TY, de Leval MR (2001) Modeling of the Norwood circulation: effects of shunt size, vascular resistances, and heart rate. Am J Physiol Heart Circ Physiol 280:H2076–H2086
13. Santamore WP, Burkhoff D (1991) Hemodynamic consequences of ventricular interaction as assessed by model analysis. Am J Physiol 260:H146–H157
14. Sagawa K, Maughan L, Suga H, Sunagawa K (1988) Cardiovascular interaction. In: Sagawa K, Maughan L, Suga H, Sunagawa K (eds) Cardiac contraction and the pressure–volume relationship. Oxford University Press, Oxford
15. Walther FJ, Siassi B, King J, Wu PY (1986) Blood flow in the ascending and descending aorta in term newborn infants. Early Hum Dev 13:21–25
16. Wang JJ, Flewitt JA, Shrive NG, Parker KH, Tyberg JV (2006) Systemic venous circulation. Waves propagating on a windkessel: relation of arterial and venous windkessels to systemic vascular resistance. Am J Physiol Heart Circ Physiol 290:H154–H162
17. McElhinney DB, Reddy VM, Hanley FL, Moore P (1997) Systemic venous collateral channels causing desaturation after bidirectional cavopulmonary anastomosis: evaluation and management. J Am Coll Cardiol 30:817–824
18. Gatzoulis MA, Shinebourne EA, Redington AN, Rigby ML, Ho SY, Shore DF (1995) Increasing cyanosis early after cavopulmonary connection caused by abnormal systemic venous channels. Br Heart J 73:182–186
19. Webber SA, Horvath P, LeBlanc JG, Slavik Z, Lamb RK, Monro JL, Reich O, Hruda J, Sandor GG, Keeton BR, Salmon AP (1995) Influence of competitive pulmonary blood flow on the bidirectional superior cavopulmonary shunt. A multi-institutional study. Circulation 92:II279–II286
20. Trusler GA, Williams WG, Cohen AJ, Rabinovitch M, Moes CA, Smallhorn JF, Coles JG, Lightfoot NE, Freedom RM (1990) William Glenn lecture. The cavopulmonary shunt. Evolution of a concept. Circulation 82:IV131–IV138
21. Gelatt M, Hamilton RM, McCrindle BW, Gow RM, Williams WG, Trusler GA, Freedom RM (1994) Risk factors for atrial tachyarrhythmias after the Fontan operation. J Am Coll Cardiol 24:1735–1741
22. Balaji S, Gewillig M, Bull C, de Leval MR, Deanfield JE (1991) Arrhythmias after the Fontan procedure. Comparison of total cavopulmonary connection and atriopulmonary connection. Circulation 84:III162–III167
23. Little WC, Ohno M, Kitzman DW, Thomas JD, Cheng CP (1995) Determination of left ventricular chamber stiffness from the time for deceleration of early left ventricular filling. Circulation 92:1933–1939
24. Lisauskas JB, Singh J, Bowman AW, Kovács SJ (2001) Chamber properties from transmitral flow: prediction of average and passive left ventricular diastolic stiffness. J Appl Physiol 91:154–162
25. Garcia MJ, Firstenberg MS, Greenberg NL, Smedira N, Rodriguez L, Prior D, Thomas JD (2001) Estimation of left ventricular operating stiffness from Doppler early filling deceleration time in humans. Am J Physiol Heart Circ Physiol 280:H554–H561
26. Gaynor SL, Maniar HS, Bloch JB, Steendijk P, Moon MR (2005) Right atrial and ventricular adaptation to chronic right ventricular pressure overload. Circulation 112:I212–I218
27. Szabó G, Buhmann V, Graf A, Melnitschuk S, Bährle S, Vahl CF, Hagl S (2003) Ventricular energetics after the Fontan operation: contractility-afterload mismatch. J Thorac Cardiovasc Surg 125:1061–1069

Basic Res Cardiol (2010) 105:787–794
DOI 10.1007/s00395-010-0119-y

ORIGINAL CONTRIBUTION

A histamine H_2 receptor blocker ameliorates development of heart failure in dogs independently of β-adrenergic receptor blockade

Hiroyuki Takahama · Hiroshi Asanuma · Shoji Sanada · Masashi Fujita · Hideyuki Sasaki · Masakatsu Wakeno · Jiyoong Kim · Masanori Asakura · Seiji Takashima · Tetsuo Minamino · Kazuo Komamura · Masaru Sugimachi · Masafumi Kitakaze

Received: 21 July 2010 / Revised: 31 August 2010 / Accepted: 2 September 2010 / Published online: 18 September 2010

Abstract Histamine has a positive inotropic effect on ventricular myocardium and stimulation of histamine H_2 receptors increases the intracellular cAMP level via Gs protein, as dose stimulation of β-adrenergic receptors, and worsens heart failure. To test whether a histamine H_2 receptor blocker had a beneficial effect in addition to β-adrenergic receptor blockade, we investigated the cardioprotective effect of famotidine, a histamine H_2 receptor blocker, in dogs receiving a β-blocker. We induced heart failure in dogs by rapid ventricular pacing (230 beats/min). Animals received no drugs (control group), famotidine (1 mg/kg daily), carvedilol (0.1 mg/kg daily), or carvedilol plus famotidine. Both cardiac catheterization and echocardiography were performed before and 4 weeks after the initiation of pacing. Immunohistochemical studies showed the appearance of mast cells and histamine in the myocardium after 4 weeks of pacing. In the control group, the left ventricular ejection fraction (LVEF) was decreased after 4 weeks compared with before pacing (71 ± 2 vs. $27 \pm 2\%$, $p < 0.05$) and mean pulmonary capillary wedge pressure (PCWP) was increased (8 ± 1 vs. 19 ± 3 mmHg). Famotidine ameliorated the decrease of LVEF and increase of PCWP, while the combination of carvedilol plus famotidine further improved both parameters compared with the carvedilol groups. These beneficial effects of famotidine were associated with a decrease of the myocardial cAMP level. Histamine H_2 receptor blockade preserves cardiac systolic function in dogs with pacing-induced heart failure, even in the presence of β-adrenergic receptor blockade. This finding strengthens the rationale for using histamine H_2 blockers in the treatment of heart failure.

Keywords Heart failure · Histamine · Histamine H_2 receptor blocker · β-Adrenergic receptor blocker

Introduction

Chronic heart failure (CHF) is one of the major causes of morbidity and mortality worldwide, and is characterized by neurohormonal imbalances that include activation of the sympathetic nervous system [9, 15]. β-Adrenergic receptor blockade is a established treatment of CHF because it protects the heart from the harmful effects of the sympathetic nervous system that are partly mediated via cyclic adenosine monophosphate (cAMP)-dependent pathways [2, 34]. Interestingly, histamine H_2 receptors are linked to Gs proteins that facilitate the production of cAMP (as are β-adrenergic receptors) and are expressed in the heart [18, 29, 33]. Histamine has a positive inotropic effect on human ventricular myocardium and chronotropic effects [3, 12], and also autonomic control of the heart [21]. Indeed, we previously reported that famotidine, a histamine H_2

H. Takahama · M. Wakeno · J. Kim · M. Asakura · M. Kitakaze (✉)
Department of Cardiovascular Medicine, National Cerebral and Cardiovascular Center, Suita, Osaka 565-8565, Japan
e-mail: kitakaze@zf6.so-net.ne.jp

H. Asanuma · H. Sasaki · K. Komamura · M. Sugimachi
Cardiovascular Dynamics Research Institute, National Cerebral and Cardiovascular Center, Suita, Japan

H. Asanuma
Department of Emergency Room Medicine, Kinki University School of Medicine, Osaka-Sayama, Japan

S. Sanada · M. Fujita · S. Takashima · T. Minamino
Department of Cardiovascular Medicine, Osaka University Graduate School of Medicine, Suita, Japan

receptor blocker, protected the heart against ischemia-reperfusion injury in dogs [1] and also improved both symptoms of CHF and ventricular remodeling in the clinical setting [16]. Although the maximum inotropic effects of substances acting through cAMP were decreased in diseased myocardium [6], famotidine, a histamine H_2 receptor blocker, exerts negative effects on cardiac performance [13], the roles of the histamine would have remained unclear in the state of heart failure.

In addition, it is still unclear whether histamine H_2 receptor blockers have a protective effect against CHF by reducing the myocardial accumulation of cAMP and whether there is an additive effect of histamine H_2 receptor blockade in the presence of β-adrenergic receptor blockade.

Therefore, we investigated the effect of a histamine H_2 receptor blocker on cardiac performance and myocardial cAMP accumulation in dogs with pacing-induced heart failure, and also investigated whether there was an additive effect of combined histamine H_2 receptor blocker and β-blocker therapy on cardiac performance.

Methods

Materials

The histamine H_2 receptor blocker famotidine was kindly provided by Astellas Pharma Inc. (Tokyo, Japan). Carvedilol, a β-adrenergic receptor blocker, was obtained from Sigma (St. Louis, MO, USA). Rabbit polyclonal anti-histamine antibody was obtained from Progen (Queensland, Australia).

Animal preparation

Beagle dogs (Oriental Yeast Co. Ltd., Tokyo, Japan) weighing 8–10 kg were sedated with intravenous sodium pentobarbital at a dose of 25 mg/kg. After intubation with a cuffed endotracheal tube, anesthesia was maintained with 0.5–1% isoflurane and an equal mixture of air and oxygen. Ventilation was provided with a tidal volume of 22 mL/kg at a rate of 15 times per minute. A bipolar pacing lead (Model BT-45P, Star Medical Inc., Tokyo, Japan) was advanced under fluoroscopic guidance through the right jugular vein to the right ventricular (RV) apex and was connected to an external programmable pacemaker (VOO mode; Model SIP-501, Star Medical Inc., Tokyo, Japan) that was implanted in a subcutaneous pocket in the neck. The success of this procedure was confirmed by electrocardiography. Antibiotics were given after surgery, and the dogs were allowed to recover fully. Then heart failure was induced by rapid right ventricular pacing at a rate of 230 beats/min for 4 weeks as the model mimicking heart failure in human, as reported previously [22, 23, 27].

All procedures were performed in conformity with the Guide for the Care and Use of Laboratory Animals (NIH publication No. 85–23, 1996 revision) and were approved by the ethical committee for laboratory animal use of the National Cardiovascular Center in Japan.

Echocardiography

Transthoracic echocardiography was performed by using an echocardiographic system equipped with a 2–4 MHz phased-array transducer (SONOS 5500, Hewlett Packard, Massachusetts, USA) in conscious dogs before pacemaker implantation and 30 min after the cessation of RV pacing at 4 weeks. Good two-dimensional short-axis views of the left ventricle were obtained at the level of the papillary muscles for guided M-mode measurement of the left ventricular (LV) end-diastolic dimension (LVDd), LV end-systolic dimension (LVDs), LV fractional shortening (LVFS), and LV ejection fraction (LVEF). All measurements were made by two observers, who were blinded to the source of the tracings.

Hemodynamic studies

LV pressure and mean aortic pressure were measured by pressure amplifiers connected to a pig tail catheter (5F, Terumo Co. Ltd., Tokyo, Japan) that was inserted into the left ventricle from the left femoral artery. Pulmonary capillary wedge pressure (PCWP) was measured with a 7 Fr Swan-Ganz catheter (American Edwards Laboratories, California, USA). LV dP/dt was analyzed using software (Data viewer, Yokogawa Electric Corporation, Tokyo, Japan). These studies were performed both before and after 4 weeks of RV pacing or 4 weeks after pacemaker implantation in the sham group.

Measurement of the myocardial cAMP level

The myocardial cyclic AMP (cAMP) level was measured as described previously [8]. Briefly, a sample of frozen cardiac muscle was homogenized mechanically in 500 mL of frozen hydrochloric acid (0.1 N) with a mechanical homogenizer. The homogenate was thawed and centrifuged at $5{,}000 \times g$ at room temperature for 15 min and then a 100 mL aliquot of the supernatant was employed to measure cAMP with a sensitive radioimmunoassay (cyclic AMP kit; Yamasa Shoyu Co., Choshi, Japan).

Immunohistochemical analysis

Immunohistochemical analysis was performed as described previously [24]. Briefly, myocardial tissue samples were fixed in 10% formalin and embedded in paraffin. Then

5-μm-thick sections were cut and preincubated with 3% hydrogen peroxide. Rabbit polyclonal anti-histamine antibody (1:1,000 dilution) was added, and incubation was done at room temperature overnight. Next, the sections were incubated with biotinylated anti-rabbit immunoglobulin for 30 min and subsequently with horseradish peroxidase-labeled streptavidin solution for 30 min. The slides were rinsed in tris-buffered saline after each incubation step. Peroxidase activity was visualized by incubation with diaminobenzidine hydrochloride solution.

Experimental protocols

Protocol 1: effects of famotidine on cardiac performance and myocardial cAMP accumulation in dogs with pacing-induced heart failure

After pacemaker implantation, the dogs were randomly assigned to a sham group ($n = 6$) without pacing, a control group ($n = 7$) with pacing only, and a famotidine group ($n = 5$) with pacing plus the daily oral administration of famotidine (1 mg/kg per day). The dose of famotidine was chosen on the basis of previous reports [30, 36]. Echocardiography and measurement of hemodynamic parameters were performed before and 4 weeks after pacemaker implantation. After the measurement of hemodynamic parameters, myocardial tissue samples were obtained and quickly placed into liquid nitrogen for storage at −80°C until measurement of cAMP levels.

Protocol 2: effects of famotidine on cardiac performance in dogs with pacing-induced heart failure under β-adrenergic receptor blockade

Next, we examined the additive effect of histamine H_2 receptor blockade on the development of CHF. After pacemaker implantation, the dogs were randomly assigned to a carvedilol group ($n = 6$) that received daily oral administration of carvedilol (0.1 mg/kg per day) or a carvedilol + famotidine group ($n = 6$) that received daily oral administration of both carvedilol (0.1 mg/kg per day) and famotidine (1 mg/kg per day).

Statistical analysis

Results are expressed as the mean ± SEM. Comparison of time-course changes between the groups was performed by two-way repeated measures analysis of variance (ANOVA). For comparison of mast cell counts and cAMP levels between the groups, the Mann–Whitney U test was performed. A p value < 0.05 was considered to represent statistical significance.

Results

Mast cells and histamine expression

Mast cells were detected in the myocardium by toluidine blue staining. Consistent with previous reports [8, 26], we observed an increase of mast cells in the failing hearts compared with the number of cells in the sham group (Fig. 1a). Immunohistochemical analysis showed an increase of histamine expression indicating increased degranulation of mast cells in failing hearts compared with the level in the sham group (Fig. 1b).

Effect of famotidine on cardiac performance and myocardial cAMP in dogs with pacing-induced heart failure

Both mean aortic pressure and heart rate before pacing were similar in the control group (104 ± 5 mmHg and

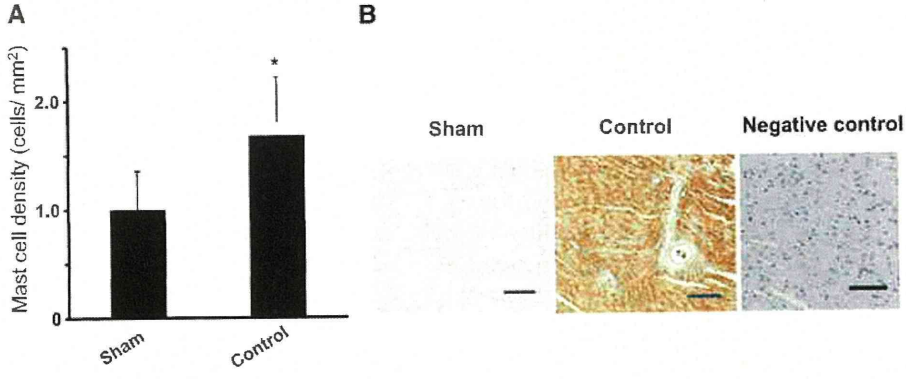

Fig. 1 Mast cell density and histamine expression in the failing heart. **a** Mast cell density in the heart. Values are the mean ± SEM. *$p < 0.05$ versus the sham group. **b** Immunostaining with an anti-histamine antibody. **a** Representative staining of a heart from the sham group. **b** Representative staining of a heart from the control group. **c** Negative control section incubated without the primary antibody. The *scale bars* indicate 50 μm

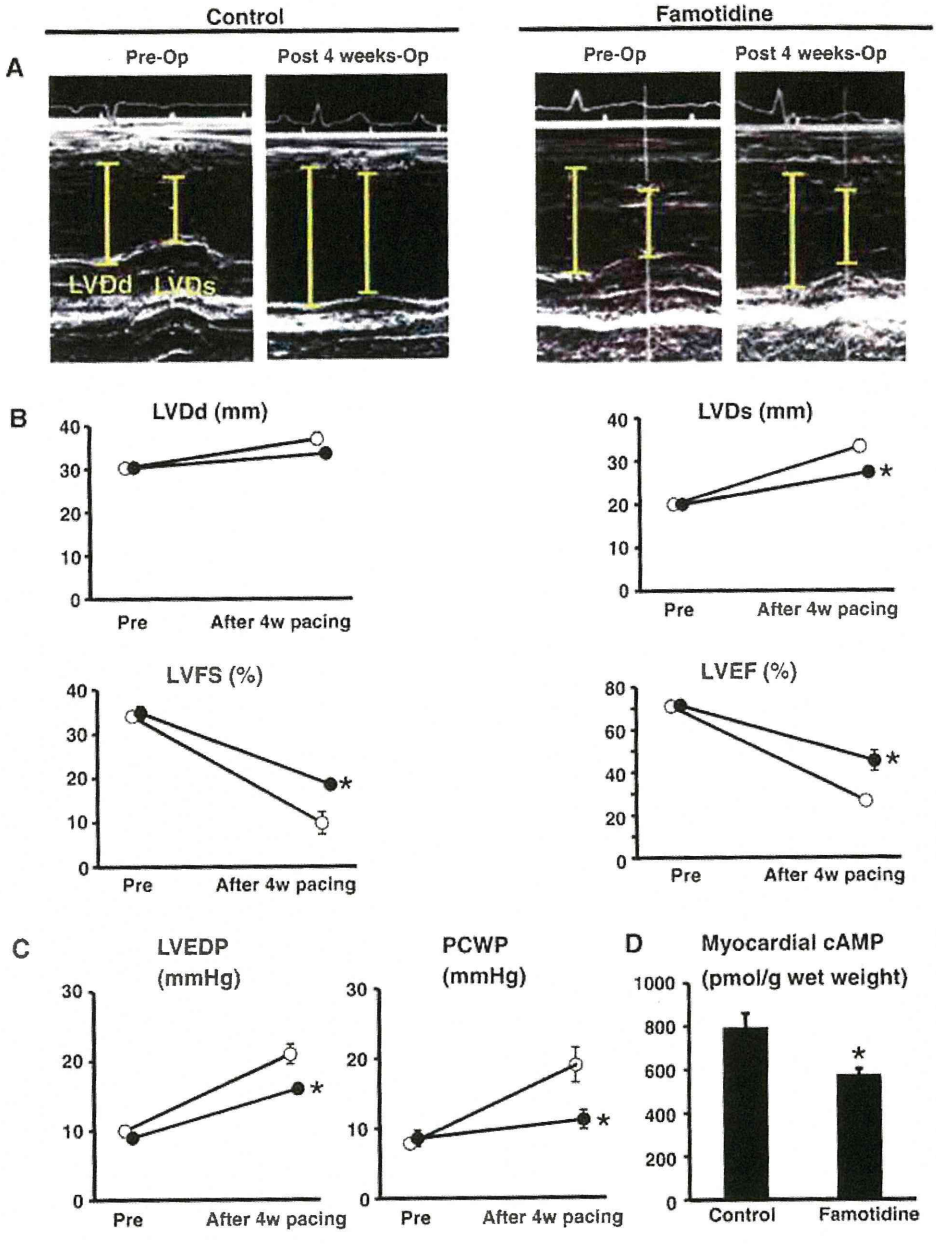

Fig. 2 Effects of famotidine on echocardiographic and hemodynamic parameters and myocardial cAMP levels. **a** Representative 2D echocardiograms. **b** Quantitative analysis of echocardiographic parameters in the control and famotidine groups. *Open* and *closed circles* indicate the control group and the famotidine group, respectively. **c** LVEDP and mean PCWP in the control and famotidine groups. **d** Myocardial cAMP levels in each group. All values are the mean ± SEM. $*p < 0.05$ versus the sham group

117 ± 7 bpm, respectively), and the famotidine group (101 ± 3 mmHg and 115 ± 8 bpm, respectively). These parameters did not significantly differ among the groups. LV d*P*/d*t* was 3,592 ± 512 mmHg/s in the control group and 3,981 ± 528 mmHg/s in the famotidine group. Four weeks after surgery, neither hemodynamic nor echocardiographic data showed any changes compared with the preoperative values in the sham group (data not shown). Four weeks after rapid RV pacing, an administration of famotidine significantly limited the increase of both LVDd and LVDs, as well as the decrease of both LVFS and LVEF (33.4 ± 0.8 mm, 27.4 ± 1.2 mm, 18.5 ± 2.6% and 45.4 ± 4.8%, respectively), compared with the findings in the control group (37.0 ± 1.4 mm, 33.4 ± 1.4 mm, 9.9 ± 1.0% and 26.7 ± 2.4%, respectively) (Fig. 2a, b). Four weeks after RV pacing, LV end-diastolic pressure (LVEDP) and PCWP of the famotidine group (16 ± 2 and 11 ± 1 mmHg, respectively), were both significantly lower compared with the values in the control group (21 ± 2 and 19 ± 2 mmHg and, respectively) (Fig. 2c). LV d*P*/d*t* after RV pacing was significantly preserved higher in the famotidine group (2,601 ± 216 mmHg/s) compared with that in control group (2,077 ± 124 mmHg/s) ($p < 0.05$).

The myocardial cAMP level was significantly higher in the control group (796 ± 111 pmol/g wet weight) compared with that in the sham group (597 ± 77 pmol/g wet

weight), while it was significantly lower in the famotidine group (577 ± 28 pmol/g wet weight) compared with the control group ($p < 0.05$) (Fig. 2d).

Additive effects of famotidine and a β-blocker on cardiac performance in dogs with pacing-induced heart failure

Before pacing, mean aortic pressure and heart rate were both similar in the carvedilol group (101 ± 7 mmHg and 111 ± 8 bpm, respectively), and the famotidine + carvedilol group (93 ± 2 mmHg, 106 ± 7 bpm, respectively), and these parameters did not significantly differ among the groups. LV d*P*/d*t* was 3,672 ± 417 mmHg/s in the carvedilol group and 3,941 ± 284 mmHg/s in the famotidine + carvedilol group. After rapid RV pacing for 4 weeks, both LVDd and LVDs were decreased and both LVFS and LVEF were increased (33 ± 0.4 mm, 25 ± 0.7 mm, 28 ± 2%, and 54 ± 3%, respectively), in the famotidine + carvedilol group compared with the respective values in the carvedilol group (34 ± 1 mm, 28 ± 1 mm, 23 ± 1%, and 38 ± 5%, respectively) (Fig. 3a).

Four weeks after RV pacing, LVEDP and PCWP of the carvedilol + famotidine group (12 ± 3 and 10 ± 4 mmHg, respectively), were both significantly reduced compared with the respective values in the carvedilol group (16 ± 2 and 15 ± 1 mmHg, respectively) (Fig. 3b). LV d*P*/d*t* after RV pacing was preserved higher in the famotidine + carvedilol group (3,382 ± 252 mmHg/s) compared with that in carvedilol group (2,740 ± 321 mmHg/s) ($p < 0.05$).

Furthermore, the myocardial cAMP level was significantly lower in the carvedilol + famotidine group (488 ± 45 pmol/g wet weight) compared with that in the carvedilol group (615 ± 28 pmol/g wet weight) (Fig. 3c).

Discussion

In the present study, we demonstrated that (1) myocardial histamine expression was increased by pacing-induced heart failure, (2) the histamine H_2 receptor blocker famotidine improved cardiac performance (gauged by echocardiographic and hemodynamic parameters) along with a reduction of myocardial cAMP accumulation, and (3) there was an additive effect of combined histamine H_2 receptor and β-adrenergic receptor blockade on cardiac performance in dogs with pacing-induced heart failure.

Impact of histamine blockade on cardiac failure

Histamine is one of the autacoids, and is stored and released by mast cells in the human heart, as well as in other organs or

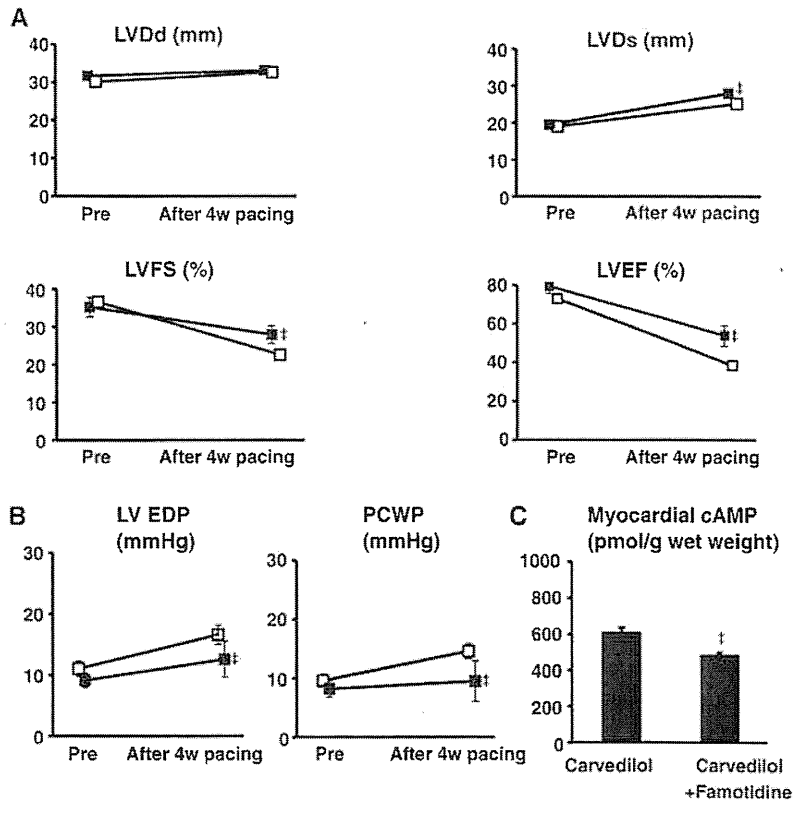

Fig. 3 Additive effect of famotidine and carvedilol on cardiac performance. **a** Quantitative analysis of echocardiographic parameters in the carvedilol and carvedilol + famotidine groups. *Open* and *closed squares* indicate the carvedilol group and the carvedilol + famotidine group, respectively. **b** LVEDP and mean PCWP in the carvedilol group and carvedilol + famotidine group. *Open* and *closed squares* indicate the carvedilol group and the carvedilol + famotidine group, respectively. **c** Myocardial cAMP levels in each group. All values are the mean ± SEM. *$p < 0.05$ versus the carvedilol group

tissues [8]. Recently, the number of mast cells and the myocardial histamine level were found to increase in the hearts of patients with idiopathic dilated cardiomyopathy or ischemic cardiomyopathy [26]. Histamine modulates various cellular functions via the activation of four different G-protein-coupled receptors (H_{1-4} receptors) [29]. As is well known, histamine H_2 receptors located on gastric cells promote the production of gastric acid [10] and histamine H_2 receptor blockers have been widely used for the treatment of peptic ulcer. Interestingly, histamine H_2 receptors are also expressed in canine and human ventricular myocardium [14, 18], although the expression levels were different among species [18]. Consisted with the previous studies, we confirmed the presence of histamine H_2 receptor in the canine heart using quantitative reverse-transcriptase PCR (data not shown).

In the present study, the precise locations of histamine receptors in myocytes or vessels in the canine hearts remained unclear. However, since famotidine did not decrease blood pressure in this study, the accumulating lines of evidence would suggest that histamine H_2 blockers did not have the potent effect on the vessels compared with cardiomyocytes. On the other hand, since histamine H_1 receptors are abundantly expressed in the vessels in most animal species [29], histamine H_1 receptor blocker has the effects on vessels. In addition, stimulation of H_2 receptors transduces the intracellular signals via Gs protein, as does the stimulation of β-adrenergic receptors. Moreover, histamine has a positive inotropic effect on human ventricular myocardium and has been suggested to have a role in cardiovascular diseases [3, 11]. Although it was reported that the maximum inotropic effects of histamine receptor stimulation were less than those mediated by beta-adrenergic receptors [5, 35], the roles of histamine receptor blockade have remained unclear compared with those of beta-adrenergic receptor.

Based on these backgrounds, we previously proposed that histamine H_2 receptor blockers could provide a novel therapeutic strategy for heart failure, and we have reported that histamine H_2 blocker treatment may have a cardioprotective effect in patients with chronic heart failure [16]. In the present study, we found that myocardial histamine expression was increased in dogs with pacing-induced heart failure compared with that in sham dogs on immunohistochemical analysis. Also, the histamine H_2 receptor blocker, famotide, prevented the development of heart failure induced by rapid RV pacing and lessened the myocardial accumulation of cAMP. These findings suggest that histamine H_2 receptor blockade exerts a cardioprotective effect along with the amelioration of myocardial cAMP accumulation. Recently it was reported that increased cardiac adenylyl cyclase expression is associated with mortality after myocardial infarction in rats [31]. It has been controversial for the role of myocardial cAMP in the heart failure [17]. Although increased cAMP acutely induced the improvement of ventricular function, several trials with either beta-adrenergic agonists or PDE inhibitors have revealed an increase in mortality [17, 20]. In the present study, in the dogs with the drugs that decreases myocardial cAMP levels, the development of heart failure was substantially attenuated, however further investigation will be needed to solve the roles of cAMP in the onset and progression of heart failure.

Additive effects of histamine H_2 blocker and β-blocker therapy on cardiac performance

β-Blockers have long been established as useful agents for chronic heart failure [2, 7, 25, 32]. These drugs act by preventing intracellular Ca overload, because β-adrenergic stimulation promotes Ca overload via Gs protein [34]. Histamine H_2 receptor blockade also prevents Ca overload [28], so we hypothesized that the combination of a histamine H_2 receptor blocker and a β-blocker would exert a stronger cardioprotective effect than either agent alone. Almost all of the patients in our earlier study, which showed that histamine H_2 receptor blockers were effective for the treatment of CHF, were also on β-blocker therapy [16], suggesting that there was an additive effect of histamine H_2 receptor and β-adrenergic receptor blockade in patients with CHF. In the present study, we demonstrated that the combination of a histamine H_2 receptor blocker and a β-blocker prevented the development of heart failure compared with β-blocker monotherapy. Thus, histamine H_2 receptor blockers have a potential clinical role in the treatment of CHF.

Rationale of the present study

The present study provided strong experimental evidence that histamine H_2 receptor blockade improves the pathophysiology of CHF. We have already reported about the beneficial effects of famotidine in patients with heart failure [16]. However, clinical research may be confounded by unexpected errors due to (1) the influence of other drugs being used by patients with CHF, (2) variation in the severity of CHF between patients, and (3) variation in the duration of CHF. Therefore, it was important to prove that histamine H_2 receptor blockade improves CHF in a controlled experimental setting (canine cardiomyopathy model) to support the clinical use of famotidine for CHF. Furthermore, to determine the merit of famotidine in heart failure patients, the present study would be a basis to design a prospective randomized double-blinded study.

Limitations

There are several limitations in this study. First, carvedilol blocks alpha$_1$-, beta$_1$-, beta$_2$- receptors, decreased the cardiac effects of norepinephrine, and has additional antioxidant and antiproliferative effects [4, 19]. In the present study, we did not address that carvedilol has the pleiotropic effects and is not just a beta-blocker.

Second, we did not measure cardiac output as a cardiac contractive index in the present study. However, we have previously reported that our tachycardia-induced heart failure model in dogs using the same procedure of the present study, revealed the low output state that mimics heart failure in human [27]. Our untreated dogs in the heart failure group were strongly suggested in the low output state because of decreased the level of ejection fraction as much as our previous study. In the present study, we analyzed the values of dP/dt as the index of contractility by measuring LV pressure using a pig tail catheter.

In summary, despite these limitations, we demonstrated that the histamine H_2 receptor blockade preserves cardiac systolic function in dogs with pacing-induced heart failure, even in the presence of β-adrenergic receptor blockade. This finding strengthens the rationale for the beneficial effects of histamine H_2 blockers in the treatment of heart failure.

Acknowledgments The authors thank Akiko Ogai for technical assistance; Masahiko Takahashi (Astellas Co. Ltd.) for providing information on famotidine; and the Evidence Finders' Club for their encouragement of this study. This work was supported by a Grant-in-aid from the Japanese Ministry of Health, Labor, and Welfare; a Grant-in-aid from the Japanese Ministry of Education, Culture, Sports, Science and Technology; a Grant from the Japan Heart Foundation; and a Grant from the Japan Cardiovascular Research Foundation.

Conflict of interest None.

References

1. Asanuma H, Minamino T, Ogai A, Kim J, Asakura M, Komamura K, Sanada S, Fujita M, Hirata A, Wakeno M, Tsukamoto O, Shinozaki Y, Myoishi M, Takashima S, Tomoike H, Kitakaze M (2006) Blockade of histamine H_2 receptors protects the heart against ischemia and reperfusion injury in dogs. J Mol Cell Cardiol 40:666–674
2. Bristow MR, Gilbert EM, Abraham WT, Adams KF, Fowler MB, Hershberger RE, Kubo SH, Narahara KA, Ingersoll H, Krueger S, Krueger S, Young S, Shusterman N (1996) Carvedilol produces dose-related improvements in left ventricular function and survival in subjects with chronic heart failure. Circulation 94:2807–2816
3. Bristow MR, Ginsburg R, Harrison DC (1982) Histamine and the human heart: the other receptor system. Am J Cardiol 49:249–251
4. Bristow MR (1997) Mechanism of action of beta-blocking agents in heart failure. Am J Cardiol 80:26L–40L
5. Brodde OE, Hillemann S, Kunde K, Vogelsang M, Zerkoski HR (1992) Receptor systems affecting force of contraction in the human heart and their alterations in chronic heart failure. J Heart Lung Transplant 11:S164–S174
6. Brown L, Lorenz B, Erdmann E (1986) Reduced positive inotropic effects in diseased human ventricular myocardium. Cardiovasc Res 20:516–520
7. CIBIS II Investigators and Committees (1999) The cardiac insufficiency bisoprolol study II (CIBIS II): a randomized trial. Lancet 353:9–13
8. Dvorak AM (1986) Mast-cell degranulation in human hearts. N Engl J Med 315:969–970
9. Eichhorn EJ (1998) Restoring function in failing hearts: the effects of beta blockers. Am J Med 104:163–169
10. Gantz I, Schaffer M, DelValle J, Logsdon C, Campbell V, Uhler M, Yamada T (1991) Molecular cloning of a gene encoding the histamine H_2 receptor. Proc Natl Acad Sci USA 88:5937
11. Hara M, Ono K, Hwang MW, Iwasaki A, Okada M, Nakatani K, Sasayama S, Matsumori A (2002) Evidence for a role of mast cells in the evolution to congestive heart failure. J Exp Med 195:375–381
12. Hattori Y (1999) Cardiac histamine receptors: their pharmacological consequences and signal transduction pathways. Methods Find Exp Clin Pharmacol 21:123–131
13. Hinrichsen H, Halabi A, Kirsch W (1990) Hemodynamic effects of different H_2-receptor antagonists. Clin Pharmacol Ther 48:302–308
14. Hill SJ, Ganellin CR, Timmerman H, Schwartz JC, Shankley NP, Young JM, Schunack W, Levi R, Haas HL (1997) International Union of Pharmacology. XIII. Classification of histamine receptors. Pharmacol Rev 49:253–278
15. Jessup M, Brozena S (2003) Heart failure. N Engl J Med 348:2007–2018
16. Kim J, Ogai A, Nakatani S, Hashimura K, Kanzaki H, Komamura K, Asakura M, Asanuma H, Kitamura S, Tomoike H, Kitakaze M (2006) Impact of blockade of histamine H_2 receptors on chronic heart failure revealed by retrospective and prospective randomized studies. J Am Coll Cardiol 48:1378–1384
17. Leineweber K, Bohm M, Heusch G (2006) Cyclic adenosine monophosphate in acute myocardial infarction with heart failure Slayer or savior? Circulation 114:365–367
18. Matsuda N, Jesmin S, Takahashi Y, Hatta E, Kobayashi M, Matsuyama K, Kawakami N, Sakuma I, Gando S, Fukui H, Hattori Y, Levi R (2004) Histamine H_1 and H_2 receptor gene and protein levels are differentially expressed in the hearts of rodents and humans. J Pharmacol Exp Ther 309:786–795
19. Metra M, Giubbini R, Nodari S, Boldi E, Modena MG, Cas LD (2000) Differential effects of beta-blockers in patients with heart failure. Circulation 102:546–551
20. Movsesian MA (1999) Beta-adrenergic receptor agonists and cyclic nucleotide phosphodiesterase inhibitors: shifting the focus from inotropy to cyclic adenosine monophosphatase. J Am Coll Cardiol 34:318–324
21. Nault MA, Milne B, Parlow JP (2002) Effects of the selective H_1 and H_2 histamine receptor antagonists loratadine and ranitidine on autonomic control of the heart. Anesthesiology 96:336–341
22. Neumann T, Heusch G (1997) Myocardial, skeletal muscle, and renal blood flow during exercise in conscious dogs with heart failure. Am J Physiol 273:H2452–H2457
23. Neumann T, Vollmer A, Schaffner TH, Hess OM, Heusch G (1999) Diastolic dysfunction and collagen structure in canine pacing-induced heart failure. J Mol Cell Cardiol 31:179–192
24. Okada K, Minamino T, Tsukamoto Y, Liao Y, Tsukamoto O, Takashima S, Hirata A, Fujita M, Nagamachi Y, Nakatani T,

Yutani C, Ozawa K, Ogawa S, Tomoike H, Hori M, Kitakaze M (2004) Prolonged endoplasmic reticulum stress in hypertrophic and failing heart after aortic constriction: possible contribution of endoplasmic reticulum stress to cardiac myocyte apoptosis. Circulation 110:705–712

25. Packer M, Coats AJ, Fowler MB, Fowler MB, Katus HA, Krum H, Mohacsi P, Rouleau JL, Tendera M, Castaigne A, Roecker EB, Schultz MK, DeMets DL, Carvedilol Prospective Randomized Cumulative Survival Study group (2001) Effect of carvedilol on survival in severe chronic heart failure. N Engl J Med 344:1651–1658
26. Patella V, Marino I, Arbustini E, Lamparter-Schummert B, Verga L, Adt M, Marone G (1998) Stem cell factor in mast cells and increased mast cell density in idiopathic and ischemic cardiomyopathy. Circulation 97:971–978
27. Sasaki H, Asanuma H, Fujita M, Takahama H, Wakeno M, Ito S, Ogai A, Asakura M, Kim J, Minamino T, Takashima S, Sanada S, Sugimachi M, Komamura K, Mochizuki N, Kitakaze M (2009) Metformin prevents progression of heart failure in dogs: role of AMP-activated protein kinase. Circulation 119:2568–2577
28. Schultz G, Rosenthal W, Hescheler J (1990) Role of G proteins in calcium channel modulation. Annu Rev Physiol 52:275–292
29. Simons FE (2004) Advances in H_1-antihistamines. N Engl J Med 351:2203–2217
30. Sugiyama A, Satoh Y, Takahara A, Nakamura Y, Shimizu-Sasamata M, Sato S, Miyata K, Hashimoto K (2003) Famotidine does not induce long QT syndrome: experimental evidence from in vitro and in vivo test systems. Eur J Pharmacol 466:137–146
31. Takahashi T, Tang T, Lai C, Roth DM, Rebolledo B, Saito M, Lew WYW, Clopton P, Hammond K (2006) Increased cardiac adenylyl cyclase expression is associated with increased survival after myocardial infarction. Circulation 114:388–396
32. The MERIT-HF Study Group (1999) Effect of metoprolol CR/XL in chronic heart failure: Metoprolol CR/XL Randomized Intervention Trial in Congestive Heart Failure (MERIT-HF). Lancet 353:2001–2007
33. Trautwein W, Hescheler J (1990) Regulation of cardiac L-type calcium current by phosphorylation and G proteins. Annu Rev Physiol 52:257–274
34. Xiao RP, Cheng H, Zhou YY, Kuschel M, Lakatta EG (1999) Recent advances in cardiac beta(2)-adrenergic signal transduction. Circ Res 85:1092–1100
35. Zeekowski HR, Broede A, Kunde K, Hillemann S, Schafer E, Vogelsang M, Michel MC, Brodde OE (1993) Comparison of the positive inotropic effects of serotonin, histamine, angiotensin II, endothelin and isoprenaline in the isolated human right atrium. Naunyn-Schemiedeberg's Arch Phamacol 347:347–352
36. Zhou R, Moench P, Heran C, Lu X, Mathias N, Faria TN, Wall DA, Hussain MA, Smith RL, Sun D (2005) pH-dependent dissolution in vitro and absorption in vivo of weakly basic drugs: development of canine model. Pharm Res 22:188–192

Early Short-Term Vagal Nerve Stimulation Attenuates Cardiac Remodeling After Reperfused Myocardial Infarction

KAZUNORI UEMURA, MD, PhD,[1] CAN ZHENG, PhD,[2] MEIHUA LI, PhD,[1]
TORU KAWADA, MD, PhD,[1] AND MASARU SUGIMACHI, MD, PhD[1]

Suita, Japan; Nankoku, Japan

ABSTRACT

Background: Vagal nerve stimulation (VS) has been suggested to be an effective adjunct to reperfusion therapy in myocardial infarction (MI). However, the effect of VS on left ventricular (LV) remodeling after reperfused MI has not been examined.

Methods and Results: We investigated the effects of early, brief VS on acute inflammatory reactions (study 1) and chronic LV remodeling (study 2) in a rabbit model of reperfused MI. In study 1, rabbits were subjected to 60-minute coronary artery occlusion followed by reperfusion alone (MI, n = 8) or treated with 24-hour VS (MI-VS, n = 8). At 24 hours after ischemia-reperfusion, MI-VS rabbits showed significantly decreased myocardial infiltration of neutrophils and reduced myocardial expressions of tumor necrosis factor-α and matrix metalloproteinase-8 and -9, compared with MI rabbits. Myocardial expression of interleukin-6 was not affected by VS. In study 2, rabbits were subjected to coronary occlusion and reperfusion alone (n = 16) or treated with VS for 3 days (n = 14). At 8 weeks after ischemia-reperfusion, MI-VS rabbits showed significantly improved LV dysfunction and dilatation, and significantly reduced infarct size, infarct wall thinning, and LV weight compared with MI rabbits.

Conclusion: Early, short-term VS attenuates LV remodeling after reperfused MI, which may be associated with suppression of acute inflammatory reactions. (*J Cardiac Fail 2010;16:689–699*)

Key Words: Hypertrophy, cardiac function, acute inflammatory response, matrix metalloproteinase.

Left ventricular (LV) myocardial remodeling that occurs after myocardial infarction (MI) leads to progressive LV dilation and eventually pump dysfunction, and is one of the major determinants of long-term survival after MI.[1] In patients with acute MI, reperfusion of the ischemic tissue is the primary therapeutic strategy, and reduction of infarct size afforded by reperfusion contributes to improved clinical outcomes.[2] However, a substantial population of patients with MI still develops LV remodeling and heart failure even after reperfusion therapy.[1,2] Therefore some novel therapeutic modality should be developed as an adjunct to reperfusion therapy to attenuate chronic LV remodeling and improve the long-term outcome of MI patients.

A previous communication from our laboratory reported that electrical stimulation of vagal nerve (VS) for 6 weeks ameliorated LV remodeling and improved survival in a rat model of non-reperfused MI.[3] A small pilot clinical study demonstrated the beneficial effect of long-term, 6-month VS on LV function in patients with heart failure.[4] Several acute phase experimental studies also indicated the cardioprotective effects of VS in myocardial ischemia-reperfusion injury.[5–7] All these results strongly suggest that VS may be an effective adjunct to reperfusion therapy in patients with MI. However, the antiremodeling effect of VS remains poorly characterized and the effect on reperfused MI has not been examined.

Inflammatory cytokines are important mediators of LV remodeling after MI. Tumor necrosis factor-α (TNF-α) is an essential cytokine that is produced in significant quantities within the infarcted myocardium very soon after MI, and contributes to LV remodeling by inducing intense local inflammatory response, matrix metalloproteinase (MMP) activities, and matrix degradation.[8,9] VS has been shown

From the [1]Department of Cardiovascular Dynamics, Advanced Medical Engineering Center, National Cardiovascular Center Research Institute, Suita, Japan and [2]Department of Cardiovascular Control, Kochi Medical School, Nankoku, Japan.

Manuscript received October 9, 2009; revised manuscript received February 19, 2010; revised manuscript accepted March 2, 2010.

Reprint requests: Kazunori Uemura, MD, PhD, Department of Cardiovascular Dynamics, Advanced Medical Engineering Center, National Cardiovascular Center Research Institute, 5-7-1 Fujishirodai, Suita 565-8565, Japan. Tel: +81-6-6833-5012 (ext. 2414); Fax: +81-6-6835-5403. E-mail: kuemura@ri.ncvc.go.jp

See page 698 for disclosure information.

1071-9164/$ - see front matter

doi:10.1016/j.cardfail.2010.03.001

to attenuate hepatic and cardiac TNF-α synthesis in splanchnic artery reperfusion injury or lethal endotoxemia.[10,11] We[12] and LaCroix et al[13] have demonstrated that VS induces expression of tissue inhibitor of MMP (TIMP)-1 and reduces active MMP-9 in ischemic myocardium. Although these findings suggest that VS favorably modulates the inflammatory reactions in MI, the effects of VS on inflammatory responses including the expression of cytokines and MMPs as well as its association with the inflammatory cell infiltrations have not been investigated in the setting of MI.

Long-term VS requires permanent implantation of the entire stimulating system.[3,4] However, hemodynamically unstable patients with acute MI are poor surgical candidates. On the other hand, early brief VS via an intravascular[14] or a transcutaneous approach[11] without compromising the hemodynamic conditions would be feasible in acute clinical settings. Taking all these together, the objective of this study was to investigate the effects of early short-term VS on LV function and myocardial structural remodeling in a rabbit model of reperfused MI and their association with acute inflammatory reactions.

Methods

Animals

We used a total of 56 Japanese white rabbits in this study (male, 2.5 to 3.0 kg). The investigation conforms with the *Guide for the Care and Use of Laboratory Animals* published by the US National Institutes of Health (NIH Publication No. 85-23, revised 1996). All protocols were approved by the Animal Subjects Committee of the National Cardiovascular Center (approval number: 8042). Rabbits were assigned to the MI group (left coronary artery occlusion and reperfusion only; n = 24), MI-VS group (left coronary artery occlusion and reperfusion plus early short-term VS; n = 22), and normal control (NC) group (no treatment; n = 10).

Implantation of Vagal Nerve Electrode

Rabbits in the MI-VS group were implanted with vagal nerve electrodes. Under general anesthesia (sodium pentobarbital, 35 mg/kg^{-1}) and mechanical ventilation, a pair of polyurethane-coated stainless steel wires for electrical stimulation was looped around the right vagal nerve in the neck region.[3] The electrode wires were tunneled beneath the skin, exited in the midscapular area, and connected to a radio-controlled pulse generator (SRG-3100, Nihon Kohden, Japan) placed in a nylon jacket. Rabbits in the MI group underwent sham surgery without implanting the electrode. The animals were allowed to recover for at least 1 week before induction of MI (Fig. 1).

Induction of MI

MI was induced in rabbits of the MI and MI-VS groups (Fig. 1). Under general anesthesia (sodium pentobarbital, 35 mg/kg^{-1}) and mechanical ventilation with room air, a left thoracotomy was performed. A 4-0 proline suture was passed around the circumflex coronary artery, and a snare was formed by passing the ends of the thread through a small vinyl tube.[12] Electrodes to record surface electrocardiogram were implanted subcutaneously. The circumflex tourniquet was tightened to completely stop blood flow as demonstrated by both electrocardiogram changes and visual blanching of the myocardium. In the MI-VS group, we started vagal nerve stimulation immediately after coronary occlusion using rectangular pulses of 1-ms duration at 20 Hz for 10 seconds every minute.[3] We adjusted the amplitude of the pulse in each animal to reduce heart rate (HR) by 10% from baseline value. Consequently, the amplitudes ranged from 2 to 8 V. In a preliminary study, we confirmed that VS at this intensity did not alter feeding behavior and did not evoke any sign of pain reaction. After 60 minutes of coronary occlusion, the tourniquet was released, allowing reperfusion in both groups. The chest wall was then closed, and the animal was allowed to recover.

After recovery from anesthesia of MI surgery, we checked HR response to VS in MI-VS rabbits by monitoring electrocardiogram at least twice per day under conscious condition. We readjusted the intensity of VS if necessary, because the response varied from day to day in an individual rabbit.

Experimental Protocols

We performed 2 studies (Fig. 1). In study 1, VS was continued for 24 hours in MI-VS rabbits, and the effects of VS on myocardial inflammatory reactions at 24 hours after coronary reperfusion were examined because myocardial expression of TNF and MMP-9 as well as infiltration of neutrophil have been shown to peak at around 24 hours after myocardial ischemia reperfusion.[15] In study 2, VS was continued for 3 days in MI-VS rabbits, and LV function and structure were examined at 8 weeks after coronary reperfusion.

Study 1: Acute Phase after MI

Study 1 consisted of 3 groups of rabbits: MI (n = 8), MI-VS (n = 8), and NC (n = 3). At 24 hours after coronary reperfusion, animals in the MI and MI-VS groups were euthanized and whole hearts were harvested.

Western Blot. Myocardial tissue sample obtained from the LV lateral wall (infarct region in MI and MI-VS rabbits) was homogenized in RIPA lysis buffer (Rockland, Gilbertsville, PA) containing proteinase inhibitor (Complete Mini, Roche, Basel, Switzerland). The homogenate was centrifuged at 4 °C at 2000*g* for 10 minutes and the resultant supernatant was further subjected to centrifugation at 12,000*g* for 20 minutes. Protein concentration of each supernatant sample was determined using a DC Protein assay kit (BioRad Hercules, CA).

Samples containing equal amounts of protein (25 μg) were separated on 15% sodium dodecyl sulfate polyacrylamide gel electrophoresis gel (Bio-Rad) and transferred onto Immobilon-P membrane (Millipore, Billerica, MA). After blocking the membranes with BlockAce (Dainippon Pharmaceutical, Japan), TNF-α was detected with polyclonal antibody for TNF-α (sc-1348, Santa Cruz, CA) and donkey-anti-goat HRP (sc-2020, Santa Cruz). Interleukin-1β (IL-1β) was detected with polyclonal antibody for IL-1β (LS-C7719, LifeSpan Biosciences, Seattle, WA) and goat-anti-rabbit HRP (sc-2004, Santa Cruz). MMP-1, MMP-7, MMP-8, and β-actin were detected using monoclonal antibodies for MMP-1 (F-67, Daiichi Fine Chemical, Japan), MMP-7 (F82, Daiichi Fine Chemical), MMP-8 (F-83, Daiichi Fine Chemical), and β-actin (sc-47778, Santa Cruz), respectively, and goat-anti-mouse HRP (sc-2005, Santa Cruz). Protein bands were visualized with ECL Plus (GE Healthcare, UK), and analyzed using a densitometric analysis software (CS Analyzer 3.0, ATTO, Japan). Band densities were standardized to β-actin, and presented as percent

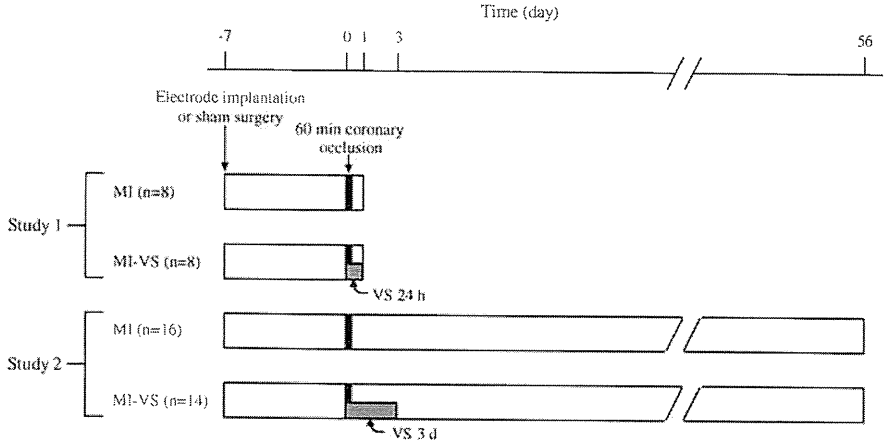

Fig. 1. Schematic representation of the protocols of Study 1 (acute phase myocardial infarction and reperfusion) and Study 2 (chronic phase after creation of reperfused myocardial infarction). MI, rabbits with reperfused myocardial infarction; MI-VS, MI rabbits treated with vagal nerve stimulation. Three rabbits in Study 1 and 7 rabbits in Study 2 were used as normal controls (not shown in this figure).

change compared with NC values, the means of which were arbitrarily set as 100%.

Enzyme-Linked Immunosorbent Assay. Myocardial tissue sample obtained from the LV lateral wall (infarct and peri-infarct regions in MI and MI-VS rabbits) was homogenized and processed as described previously.

Enzyme-linked immunosorbent assays for C-reactive protein (CRP) (KT-097, Kamiya Biomedical Company, Seattle, WA) and TIMP-1 (RPNJ409, Daiichi fine chemical) were performed using the supernatants of myocardial tissue homogenates from the infarct region according to the manufactures' instructions.[12] Enzyme-linked immunosorbent assays for IL-6 (900-033, Assay Designs, Ann Arbor, MI) was performed using the supernatants of myocardial tissue homogenates from the peri-infarct region. The reason for using the peri-infarct region instead of the infarct region for IL-6 measurement was based on a previous finding that IL-6 mRNA is intensely induced in myocytes of the viable border zone, and not the necrotic infarct zone in myocardial ischemia-reperfusion.[16]

Gelatin Zymography. Tissue sample from the LV lateral wall was homogenized in lysis buffer (50 mM Tris, pH 7.4). The homogenate was centrifuged at 2000*g* for 10 minutes at 4 °C and the supernatant was collected. Protein concentration of each supernatant sample was determined as described previously.

Gelatin zymography was performed to assess the relative contents of the gelatinases MMP-2 and MMP-9 as described previously.[12] The supernatants (30 μg protein) were loaded in Novex gels containing 0.1% gelatin (Invitrogen, Carlsbad, CA) and then electrophoresed. After renaturation, equilibration, and incubation for 20 hours at 37 °C in developing buffer, the gels were stained in 0.5% Coomassie Blue G-250. Gels were dried and scanned. MMP-2– and MMP-9–related bands were analyzed using the densitometric analysis software.

Determination of Neutrophil Infiltration. The middle ring slice of LV was embedded in paraffin, sectioned at a thickness of 5 μm, and stained with hematoxylin and eosin. We counted the numbers of neutrophils per field in the infarcted area. Neutrophil infiltration into ischemic myocardium was also quantified by evaluating myeloperoxidase activity. Tissue sample from the LV lateral wall was homogenized in potassium phosphate buffer (50 mM, pH 6.4) containing 0.5% hexadecyltrimethylammonium bromide (WAKO, Japan). The homogenate was centrifuged at 4 °C at 12,000*g* for 10 minutes and the resultant supernatant was reacted with 0.167 mg/mL of o-dianisidine dihydrochloride (Sigma-Aldrich, St. Louis, MO) and 0.0005% H_2O_2 in potassium phosphate buffer. The change in absorbance at 450 nm was measured spectrophotometrically over 2 minutes. One unit of myeloperoxidase activity was defined as that quantity of enzyme that hydrolyzed 1 μM of peroxide per minute at 25 °C.

Study 2: Chronic Phase after MI

Study 2 consisted of 3 groups of rabbits: MI (n = 16), MI-VS (n = 14), and NC (n = 7).

Echocardiography. Echocardiography was performed under conscious condition at baseline and at 3 days and 8 weeks after coronary reperfusion. Two-dimensional, targeted M-mode tracings were obtained at the level of the papillary muscles with an echocardiographic system equipped with a 7-MHz transducer (Power Vision, TOSHIBA, Japan). LV dimensions were measured according to the American Society for Echocardiography leading-edge method for at least 3 consecutive cardiac cycles. Fractional shortening was calculated as (LVEDD-LVESD)/LVEDD×100, where LVEDD is LV end-diastolic diameter and LVESD is LV end-systolic diameter.

Hemodynamic and Plasma MMPs Measurements. Hemodynamic measurements were performed at 8 weeks after reperfusion. Under general anesthesia (sodium pentobarbital, 35 mg/kg^{-1}) and mechanical ventilation with room air, a 3F micromanometer-tipped catheter (Millar Instruments, Houston, TX) was inserted into the right carotid artery for measurement of mean arterial pressure. Next, the catheter was advanced into the LV for measurement of LV pressure. After completing these measurements, blood was sampled from the right carotid artery. The animal was euthanized. The whole heart was quickly excised and washed with cold phosphate-buffered saline.

Relative protein contents of MMP-2 and MMP-9 in plasma were measured with use of the gelatin zymography as described previously.

LV Passive Pressure-volume Relationship. The excised heart was perfused with a cold, hypocalcemic, hyperkalemic cardioplegic solution (NaCl: 130 mM, KCl: 20 mM, $CaCl_2$: 0.08

mM, lidocaine: 0.5 μg/mL; pH 7.3; 310 mOsm). The passive LV pressure-volume relationship of the arrested heart was measured as described previously.[17] In brief, a compliant water-filled latex balloon tied on a rigid Y-connector was placed in the left ventricle and secured at the mitral annulus with a purse-string suture. Pressure within each balloon was measured with a catheter-tipped micromanometer (Millar Instruments) as volume was progressively increased. Pressure was then plotted as a function of volume at each step, resulting in a passive pressure-volume relationship equivalent to the end-diastolic pressure-volume relationship of the beating heart.[17] The size of the left ventricle was indexed by the volume at which LV pressure reached 10 mm Hg (LVV_{10}).

Infarct Characterization. The coronary branch was reoccluded and 5 mL 0.25% Evans blue was injected from the aorta at 80 mm Hg. After the vasculature, right ventricular free wall, and atrial appendages were dissected, the left ventricle was weighed and fixed in 4% paraformaldehyde overnight. The left ventricle below the coronary artery ligation site was cut into ~5 transverse slices parallel to the atrioventricular ring. Each slice was photographed. The risk area unstained by the blue dye and the non-risk area stained by the blue dye were demarcated. For each slice, the risk area size was determined as the total circumference of the risk area divided by total LV circumference (in percent). The risk area sizes of all slices were averaged and expressed as the risk area size for each heart. The fixed slices from the apex, middle ring, and base were then embedded in paraffin and sectioned at a thickness of 5 μm.

The 5-μm thick cross-sections of left ventricle were stained with Masson's trichrome and Sirius red. Using sections stained with Masson's trichrome, infarct size was determined as the total infarct circumference divided by total LV circumference (in percent). The thicknesses of septal (non-infarct area) and LV lateral walls (infarct area) were measured. The thinning ratio, an index of the extent of wall thinning in the infract, is calculated by dividing the infarct wall thickness by septal wall thickness. Cardiomyocyte cross-sectional areas were determined in the non-infarcted septal myocardium. Only cardiomyocytes cut in cross section were measured. Using sections stained with Sirius red, collagen densities in noninfarcted regions were determined as described previously.[18] Histological images were obtained with a microscope system (BZ 9000, Keyence, Japan), and analyzed using the National Institutes of Health Image software (Image J 1.37). The infarct sizes of the 3 sections (apex, middle ring, base) were averaged and expressed as the LV infarct size for each heart. The thickness of LV wall, cardiomyocyte cross-sectional area, and collagen density were determined in the section that most clearly transverses the infarct region.

Statistical Analyses

All data are presented as mean ± SEM values. Mortalities in the MI and MI-VS groups were compared using chi-square test. Between-group comparison of means obtained at a single time point was performed by Student's unpaired *t*-test or 1-way analysis of variance. Between-group comparisons of the changes of means over time were conducted using two-way repeated measure analysis of variance to examine any group-time effect. All analyses of variance showing significant differences were further analyzed by post hoc comparison using Student-Newman-Keuls test (Statistica, Statsoft, Inc., Tulsa, OK). *P* values less than .05 were considered statistically significant.

Results

Study 1: Acute Phase after MI

Body Weight and Mortality. Baseline body weight were comparable among the NC (2490 ± 38 g), MI (2656 ± 64 g), and MI-VS (2517 ± 31 g) groups. Two MI and 2 MI-VS rabbits died from arrhythmia at MI induction. There was no difference in mortality rate up to 24 hours after coronary reperfusion between the MI and MI-VS groups (25% vs. 25 %, P = NS).

HR. Changes of HR over time are summarized in Table 1. There were no significant differences in HR between the MI and MI-VS groups at baseline, after 30 minutes of coronary occlusion, and at 24 hours after coronary reperfusion. No significant time effects on HR were observed.

Myocardial Expression of Cytokines, MMPs, and CRP. Figure 2A shows representative Western blots for TNF-α in the infarcted myocardium. Densitometric analysis demonstrated that TNF-α protein level increased significantly in the MI and MI-VS groups compared with NC value, whereas TNF-α level in the MI-VS group was significantly lower than that in the MI group (<50%, $P < .05$, Fig. 2A). Myocardial protein expressions of IL-1β and IL-6 are summarized in Table 2. There were no significant differences in IL-1β level among the 3 groups. Myocardial levels of IL-6 increased significantly to similar degrees in the MI and MI-VS groups compared with NC values.

As shown in Fig. 2B, zymography of the myocardial extracts detected 2 bands at 92 kDa and 72 kDa corresponding to pro-MMP-9 and pro-MMP-2, respectively. In 2 of 11 MI hearts, but in none of 10 MI-VS hearts, a faint gelatinolytic band was also observed at 83 kDa, which presumably represents the active form of MMP-9.[19] To evaluate the relative content of MMP-9, we used the 92 kDa band (pro-MMP-9) because this band is representative of the global MMP-9 activity.[20] Relative MMP-9 level increased significantly in the MI and MI-VS groups compared with NC value. Level of MMP-9 in the MI-VS group was significantly lower than that in the MI group (<40%, $P < .05$, Fig. 2B). There were no significant differences in MMP-2 (pro-MMP-2) protein level among the 3 groups. Western

Table 1. Changes of Heart Rate with Time after Myocardial Ischemia-reperfusion (Studies 1 and 2)

	Baseline	30 Minutes	24 Hours	3 Days
Study 1				
MI	(n = 6)	277 ± 8	244 ± 24	257 ± 12
MI-VS	(n = 6)	256 ± 8	243 ± 6	250 ± 7
Study 2				
MI	(n = 11)	268 ± 10	245 ± 10	309 ± 11*†
MI-VS	(n = 10)	264 ± 22	224 ± 11	313 ± 15†

MI, myocardial infarction; MI-VS, myocardial infarction treated with vagal nerve stimulation; 30 minutes, 30 minutes after coronary occlusion; 24 hours, 24 hours after coronary reperfusion; 3 days, 3 days after coronary reperfusion.

Heart rate data (beat/min) are means ± SEM.

*$P < .05$ versus baseline.

†$P < .01$ versus 30 minutes.